MANSOURA JOURNAL OF CHEMISTRY
Official Journal of Faculty of Science, Mansoura University, Egypt
E-mail: scimag@mans.edu.eg ISSN: 2974-4938

The estimated solvation parameters for the interaction of manganese with favipiravir ligand electrochemically

M.S. Samy [a] , E.A. Gomaa [a] , M.N. Abd El-Hady [a] , H.M. Abou El Nadar [a]

[a] *Chemistry Department, Faculty of Science, Mansoura university, Egypt*

Received:5/11/2022
Accepted:13/11/2022

Abstract The electrochemical behavior of manganese ion was studied in the absence and presence of favipiravir drug at 305.15 K by cyclic voltammetry technique using glassy carbon electrode (GCE) as working electrode with surface area equal 0.0314 cm^2, Pt wire with diameter 0.5 mm as an auxiliary electrode and Ag/AgCl as a reference electrode in 0.1 M KCl (30 ml) as supporting electrolyte to balance the charge transfer. Also, to control the speed at which a potential is scanned, different scan rates (0.01, 0.02, and 0.1) $V.s^{-1}$ were carried out. A high current is observed when scan rates are faster because the diffusion layer size decreases.

keywords: Favipiravir, Cyclic voltammetry, Stability constant.

1.Introduction

Metal ions are essential components for biochemical reactions in the human body [1]. Mn has an important role in the regulation of the functions of the immune system, energy of cells, sugar of the blood, blood coagulation, digestion, reproduction, growth of bone, and resistance to reactive oxygen species (ROS) [2]. Thus, it is important to take Mn in our daily food [3,4].

Mn(II) has a half-filled $3d^5$ shell that makes it spherically polarizable, without crystal-field stabilization energy [5]. science 1966, Mn is used in combination with vitamin B1 for the effective treatment of psoriasis [6]. Recently, It was found that Mn-porphyrin complexes are potent antioxidants against superoxides ($O_2^{\cdot}$) [7].

In this article, we study the redox behavior of Mn(II)/(IV) system also, the formation of the complex between Mn and favipiravir drug (antiviral agent) electrochemically using cyclic voltammetry technique by calculating the stability constant of complex formation in solution and Gibbs free energy change.

1.Experimental

2.1. Chemicals and reagents

The chemicals used such as $MnCl_2.4H_2O$ and KCl were provided by Sigma Aldrich and absolute ethanol from Merck. The ligand (L) is a Favipiravir drug that is employed as an antiviral agent against the influenza virus [8,9] and has recently, been used as a drug for coronavirus disease [10].

2.2. Equipment

The DY 2000 Potentiostat Multichannel apparatus was used to measure the voltammograms. connected with a cell that has 3 types of electrodes (Ag/AgCl) electrode act as a reference electrode, (GCE) as a working electrode, and (Pt) wire used as an auxiliary electrode. N_2 gas was passed before each run to remove oxygen gas.

2.Result and discussion

3.1. Cyclic voltammetry equation

The kinetic, solvation and thermodynamic parameters for each voltammogram were estimated as follows:

i. The diffusion coefficient is estimated using the Randles-Sevick equation (1) which indicates the relation between the peak current i_p in Ampere and the square root of the scan rate [11-14].

$$i_p = 0.4463nFAC\left[\frac{nF\nu D}{RT}\right]^{1/2} \quad (1)$$

Where, (n) is the number of electrons transferred in the redox process, (F) is the Faraday constant which equals 96485.33 $Columbus.mol^{-1}$, (A) is the surface area of the working electrode in cm^2, and (C) is the bulk concentration of the analyte in $mol.cm^{-3}$, (D) is

the diffusion coefficient of the oxidized analyte in $cm^2.s^{-1}$, (ν) is the scan rate in $v.s^{-1}$, and (R) is the gas constant which equals 8.314 $J.mol^{-1}.K^{-1}$ and (T) is the absolute temperature in K.

ii. The potential difference between the anodic and the cathodic potentials was estimated by equation (2) [15, 16].

$$\Delta E_p = E_{pa} - E_{pc} \quad (2)$$

The heterogeneous rate constant (K_s) was calculated by applying equation (3) [17-19]. Where, (α) is the charge transfer coefficient (Assuming that its value is equal to 0.5) and n_a is the number of electrons transfer in the rate-determining step. αn_a quantity can be calculated by equation (4) [15].

$$K_s = 2.18[D_c\ \alpha n_a\ F\ \nu / RT]^{1/2} * \exp\left[\frac{\alpha^2 nF\ \Delta E_p}{RT}\right] \quad (3)$$

$$\alpha n_a = 1.857\ RT / (E_{pc} - E_{pc}/2)\ F \quad (4)$$

iii. the surface coverage Γ (surface concentration of the electroactive species in $mol.cm^{-2}$) can be calculated by equation (5) [11].

$$\Gamma = i_p\ 4RT / n^2\ F^2\ A\ \nu \quad (5)$$

The quantity of charge consumed during the redox process (Q) can be calculated by equation (6) [16].

$$Q = n\ FA\ \Gamma \quad (6)$$

vi. The stability constants (β_{MX}) for the interaction between the metal ion and ligand to form a complex are calculated by applying equation (7) [20, 21].

$$\Delta E^\circ = E^\circ_C - E^\circ_M = 2.303\ (RT/n\ F) * [\log \beta MX + j \log C_x] \quad (7)$$

Where (E°_M) is the formal peak potential of the last addition of metal before adding the ligand, (E°_C) is the formal peak potential at each addition of ligand, (j) is the coordination number of the stoichiometric complex and (C_x) is the concentration of ligand in the solution.

vii. The formal potential (E°) is calculated by equation (8) [22].

$$E^\circ = (E_{pa} + E_{pc})/2 \quad (8)$$

viii. The Gibbs free energy (ΔG) for the interaction between the metal ion and the ligand is calculated from the stability constant using equation (9) [21].

$$\Delta G = -2.303\ RT \log \beta_{MX} \quad (9)$$

3.2. The electrochemical behavior of manganese ion in absence of favipiravir ligand at 305.15K

The redox behavior of manganese chloride solution 0.05 M was studied in 0.1 M KCl (30 ml) as a supporting electrolyte at 305.15 K using the CV technique within the potential window range from 1.4 V to -0.5 v for the reduction process and the opposite scale for the oxidation process at GCE. As shown in **Fig. 1**. The resulting voltammogram had three anodic peaks, the first anodic peak A1 appear at 0.239V due to the oxidation of Mn (II) to Mn (III), the second anodic peak A2 may be due to the hydrolyses of Mn (III) to form the intermediate MnOOH and the third anodic peak A3 appear at 0.967 V due to the oxidation of MnOOH to MnO_2. And two cathodic peaks, the first cathodic peak C1 appear at 0.789 V due to the reduction of MnO_2 to MnOOH and the second cathodic peak C2 appear at 0.007 V due to the reduction of Mn (III) to Mn (II) according to the following equation [1, 23, 24].

$$Mn^{+2} \rightleftarrows Mn^{+3} + e^-$$

$$Mn^{+3} + 2H_2O \rightarrow MnOOH + 3H^+$$

$$MnOOH \rightleftarrows MnO_2 + H^+ + e^-$$

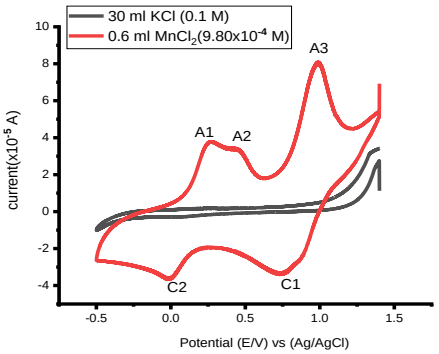

Fig. 1. *cyclic voltammogram of 0.1 M KCl and [9.80 x10^{-4}] M manganese chloride*

3.3.Effect of different concentrations of manganese at 305.15 K and scan rate 0.1 $V.s^{1-}$

The manganese chloride solution is added gradually until reach the final concentration [9.80 x10^{-4} M] as shown in **Error! Reference source not found.**. We observed that by increasing the concentration of manganese ions, the intensities of peak current (ip_a,ip_c)

gradually increase. Moreover, (Γ_c, Q_c, Γ_a and Q_a) also increased for the first and second redox peaks as presented in **Tables 1& 2**, this proved that at higher concentrations, there are a large number of electroactive species and the charge transfer process is diffusion controlled. Also, the peak current ratio (ipa\ipc) does not equal unity which indicates that the system is quasi-reversible [1].

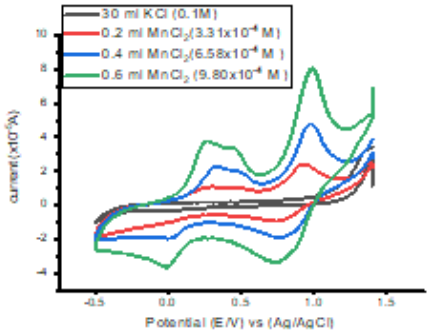

Fig. 2. Effect of different concentrations of manganese chloride at 305.15 K and scan rate 0.1V.s^{-1}.

3.3. Effect of different scan rates at last addition of manganese chloride in absence of favipiravir ligand.

A series of cyclic voltammograms of [9.80x10^{-4}] M manganese chloride was studied in 30 ml KCl [0.1] M as supporting electrolyte at several scan rates (0.1, 0.02 and 0.01) V.s^{-1} and 305.15 K as shown in **Fig. 3** . We observed that the redox peaks currents (ip_a and ip_c) decrease by decreasing of scan rate but different solvation parameters such as (Γ_c, Q_c, Γ_a and Q_a) increase by decreasing of scan rate as shown in **Tables 3& 4**. From The Randles-Sevick equation (1) the linear relation between the square root of scan rate ($\nu^{1/2}$) with peak current (ip_a and ip_c) as shown in **Figs. 4& 5**, confirm that the charge transfer process of the redox species (Mn^{+2}/Mn^{+4}) is diffusion-controlled [13].

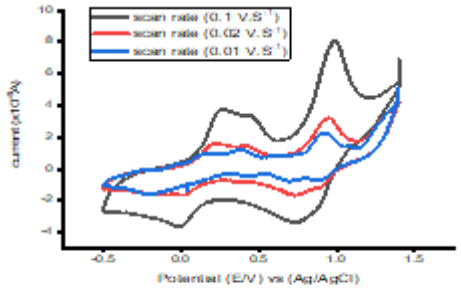

Fig. 3. Effect of different scan rates of [9.80x10^{-4}] M manganese free at 305.15

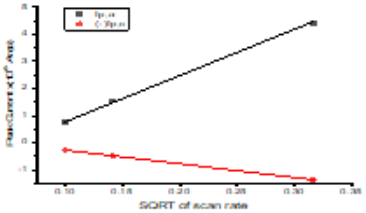

Fig. 4. The relation between (ipa and ipc) vs ($\nu^{1/2}$) of manganese alone for first redox peaks ($Mn^{4+} \rightleftarrows Mn^{3+}$).

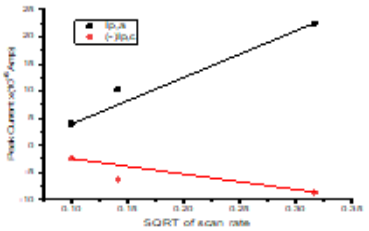

Fig. 5. The relation between (ipa and ipc) vs ($\nu^{1/2}$) of manganese alone for second redox peaks ($Mn^{3+} \rightleftarrows Mn^{2+}$).

3.3. Effect of different concentrations of favipiravir drug on the electrochemical behavior of manganese

The electrochemical behavior of manganese [9.80x10^{-4}] M was studied during the addition of favipiravir drug 0.01 M gradually in 30 ml KCl 0.1M as supporting electrolyte until reached [22.7x10^{-4}] M with 1M: 3L molar ratio at 305.15 K with potential window range from 1.4 V to -0.5 V and scan rate 0.1V.s^{-1} as shown in **Fig. 6**.

At low concentrations of favipiravir drug, there is no influence but by increasing the concentration of favipiravir gradually, the potentials shift to new values followed by decreasing in both (ip_a and ip_c) and solvation parameters such as (Γ_c, Q_c, Γ_a, and Q_c) also decrease due to the lowering of charge transfer velocity suggesting the complexation between manganese ions and favipiravir ligand as noticed in **Tables 5& 6**.

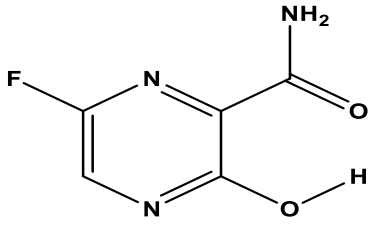

6-fluoro-3-hydroxypyrazine-2-carboxamide
Molecular Weight: 157.1

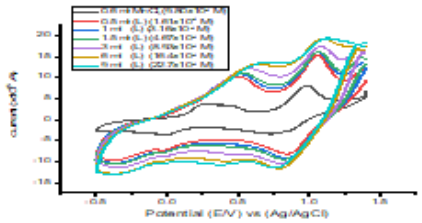

Fig. 6. Effect of different concentrations of favipiravir ligand (L) on the redox behavior of manganese at 305.15 K and scan rate 0.1V.s^{-1}

3.6. Effect of different scan rates in the presence of (Mn^{2+}-favipiravir) with molar ratio (1M:1L)

The effect of different scan rates (0.1, 0.02 and 0.01) V.s^{-1} was studied for 1M:1L molar ratio as shown in **Fig. 7**. It is observed that by decreasing of the scan rate, the value of redox peaks currents (ip_a and ip_c) and the heterogeneous rate constant (Ks) decrease, but the solvation parameters like ((Γ_c, Q_c, Γ_a and (-) Q a) increase as shown in **Tables 7& 8**. The linear relation between the (ip_a and ip_c) and **($v^{1/2}$)** confirmed that the reaction follows a diffusion controlled as shown in **Figs. 8 &9** for the first and second redox peaks.

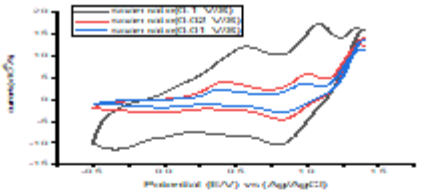

Fig. 7. Effect of different scan rates for 1M:1L molar ratio of (Mn-favipiravir) complex.

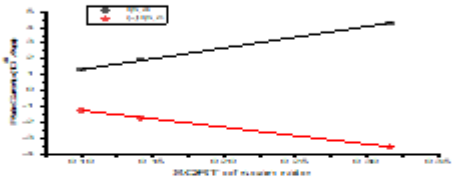

Fig. 8. The relation between (ipa and ipc) vs ($v^{1/2}$) of 1M:1L molar ratio of (Mn-favipiravir) complex for first redox peak.

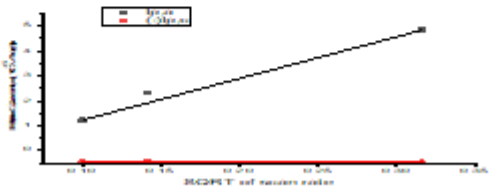

Fig.9. The relation between (ipa and ipc) vs ($v^{1/2}$) of 1M:1L molar ratio of (Mn-favipiravir) complex for second redox peak.

3.7. Study of the stability constant and Gibbs free energy change for (Mn-favipiravir) complex

When metal complexes are formed in an aqueous media, the stability constant is calculated to determine how strongly ligands and metal interact to form complexes [25].

CV technique was used to calculate The overall stability constants by finding the peak potential shift with increasing ligand concentration [19].

We observed that values of stability constant (Log βj) increase by increasing the coordination number (j) ratio, indicating the strength of the interaction between manganese and favipiravir drug toward the formation of the complex. Also, the Gibbs free energy change (ΔG) increases and has a negative value indicating that the reaction between manganese and favipiravir is a spontaneous process for the first and second redox peaks as shown in **Tables 9& 10**.

Also, the effect of different scan rates was studied on the stability constant and Gibbs free energy change. It is observed that by decreasing the scan rate, the stability constant (Log βj) and

Conclusion

The kinetic and solvation parameters of the interaction between manganese ion and favipiravir drug were calculated at 305.15K through the cyclic voltammetry technique also, the stability constant (βj) and Gibbs free energy change (ΔG) were evaluated, it is observed that values of stability constant increase by increasing the coordination number (j) ratio, indicating the strength of the interaction between manganese and favipiravir ligand toward the formation of the complex. Also, the Gibbs free energy change increased and have a negative value indicating that the reaction between manganese and favipiravir is a spontaneous process for the first and second redox peaks.

Table 1: Results of different concentrations of manganese on the kinetic and solvation parameters for first redox peaks ($Mn^{4+} \rightleftarrows Mn^{3+}$) at 305.15K and scan rate 0.1V.s^{-1}

[M]x10^{-7} mol/cm3	Ep_a Volt	Ep_c Volt	ΔEp Volt	ip_a x10^{-5} Amp	ip_cx10^{-5} Amp	ip_a/ip_c	E' Volt	$Ep_c/2$	Dax10^{-5} cm^2.s^{-1}	Dcx10^{-5} cm^2.s^{-1}	αn_a	Ks C x10^{-2} cm.s^{-1}	Γ cx10^{-9} mol.cm^{-2}	(-)Qc x10^{-5}C	Γ ax10^{-9} mol.cm^{-2}	Q_ax10^{-5} C
3.31	0.908	0.789	0.119	1.06	0.531	2.001	0.8485	0.854	14.7823	3.69	0.751	6.94	1.84	0.558	3.69	1.12
6.58	0.945	0.813	0.132	2.58	0.855	3.011	0.879	0.892	22.054	2.43	0.618	5.78	2.97	0.900	8.94	2.71
9.80	0.967	0.789	0.178	4.40	1.37	3.203	0.878	0.876	28.9894	2.83	0.561	9.20	4.77	1.45	15.28	4.63

Table 2: Results of different concentrations of manganese on the kinetic and solvation parameters for second redox peaks ($Mn^{3+} \rightleftarrows Mn^{2+}$) at 305.15K and scan rate 0.1V.s^{-1}

[M]x10^{-7} mol/cm3	Ep_a Volt	Ep_c Volt	ΔEp Volt	ip_ax10^{-5} Amp	(−)ip_cx 10^{-5} Amp	ip_a/ip_c	E' Volt	$Ep_c/2$	Dax10^{-5} cm^2.s^{-1}	Dcx10^{-5} cm^2.s^{-1}	αn_a	Ks C x10^{-1} cm.s^{-1}	Γ cx10^{-9} mol.cm^{-2}	(-) Qc x10^{-5}C	Γ ax10^{-9} mol.cm^{-2}	Q_ax10^{-5} C
3.31	0.257	0.039	0.218	0.457	0.137	3.34	0.148	0.063	2.74	0.246	2.03	0.756	0.476	0.144	1.59	0.481
6.58	0.29	0.025	0.265	1.16	0.416	2.79	0.1575	0.065	4.46	0.576	1.22	1.40	1.445	0.438	4.02	1.22
9.80	0.239	0.007	0.232	2.25	0.870	2.58	0.123	0.052	7.55	1.13	1.09	1.35	3.019	0.915	7.79	2.36

Table 3: Results of different scan rates on the kinetic and solvation parameters of 9.80x10^{-4} M $MnCl_2$ at 305.15K for first redox peaks (Mn^{4+} Mn^{3+}).

υ V.S^{-1}	Ep_a volt	Ep_c volt	ΔEp volt	ip_ax10^{-5} Amp	Qip$_c$x10^{-5} Amp	ip_a/ip_c	E' Volt	$Ep_c/2$	Da x10^{-5} cm^2.s^{-1}	Dc x10^{-5} cm^2.s^{-1}	αn_a	Ks C x10^{-2} cm.s^{-1}	Γ cx10^{-9} mol.cm^{-2}	(-) Qc x10^{-5}C	Γ ax10^{-9} mol.cm^{-2}	Q_ax10^{-5}C
0.1	0.967	0.789	0.178	4.40	1.37	3.20	0.878	0.876	29.0	2.83	0.561	9.20	4.77	1.45	15.28	4.63
0.02	0.921	0.776	0.145	1.55	0.474	3.28	0.8485	0.828	18.1	1.68	0.939	3.00	8.23	2.49	26.31	7.97
0.01	0.879	0.715	0.164	0.758	0.266	2.85	0.797	0.925	8.59	1.06	0.233	1.00	9.23	2.80	26.97	8.17

Table 4: Results of different scan rates on the kinetic and solvation parameters of 9.80 x10^{-4} M $MnCl_2$ at 305.15K for second redox peaks(Mn^{3+} Mn^{2+})

υ V.S^{-1}	Ep_a volt	Ep_c volt	ΔEp volt	ip_a x10^{-6} Amp	(-)ip_c x10^{-6} Amp	ip_a/ip_c	E' Volt	$Ep_c/2$	Da x10^{-5} cm^2.s^{-1}	Dc x10^{-5} cm^2.s^{-1}	αn_a	Ks C x10^{-2} cm.s^{-1}	Γ c x10^{-9} mol.cm^{-2}	(-) Qc x10^{-5} C	Γ a x10^{-9} mol.cm^{-2}	Q_a x10^{-5} C
0.1	0.239	0.007	0.232	2.25	0.870	2.58	0.123	0.052	7.55	1.13	1.085	13.5	3.019	0.915	7.799	2.36
0.02	0.203	0.047	0.156	1.03	0.627	1.64	0.125	0.095	7.88	2.95	1.017	4.59	8.299	2.51	13.96	4.23
0.01	0.152	-.162	0.314	0.402	0.239	1.68	0.005	-0.126	2.42	0.855	1.356	9.06	10.891	3.30	17.82	5.40

Table 5: The kinetic and solvation parameters using different concentrations of favipiravir ligand (L) for first redox peaks at 305.15 K and scan rate 0.1V.s^{-1}

[M] x10^{-7} mol/cm3	[L] x10^{-7} mol/cm3	Ep_a volt	Ep_c volt	ΔEp volt	ip_a x10^{-5} Amp	(−)ip_c x10^{-5} Amp	ip_a/ip_c	E' volt	$Ep_c/2$	Da x10^{-4} cm^2.s^{-1}	Dc x10^{-4} cm^2.s^{-1}	αn_a	Ks C x10^{-1} cm.s^{-1}	Γ c x10^{-8} mol.cm^{-2}	(-) Qc x10^{-5} C	Γ a x10^{-8} mol.cm^{-2}	Q_a x10^{-5} C
9.65	1.61	1.04	0.884	0.156	5.90	4.26	1.39	0.962	0.951	5.38	2.80	0.729	2.68	1.48	4.48	2.05	6.20
9.49	3.16	1.01	0.897	0.113	5.19	4.13	1.26	0.9535	0.95	4.29	2.72	0.921	1.97	1.43	4.34	1.80	5.46
9.35	4.67	1.05	0.856	0.194	5.15	3.52	1.46	0.953	0.926	4.36	2.04	0.698	3.21	1.22	3.70	1.79	5.41
8.93	8.93	1.06	0.839	0.221	4.28	3.47	1.23	0.9495	0.908	3.30	2.17	0.708	4.31	1.20	3.65	1.49	4.50
8.20	16.4	1.07	0.811	0.259	3.38	3.41	0.991	0.9405	0.913	2.45	2.49	0.479	5.45	1.18	3.59	1.17	3.56
7.58	22.7	1.1	0.824	0.276	3.00	3.05	0.983	0.962	0.883	2.25	2.33	0.828	8.14	1.06	3.21	1.04	3.15

Table 6: The kinetic and solvation parameters using different concentrations of favipiravir ligand for second redox peaks at 305.15 K and scan rate 0.1V.S^{-1}

[M]x10^{-7} mol/cm3	[L] x10^{-7} mol/cm3	Ep_a volt	Ep_c volt	ΔEp volt	ip_a x10^{-6} Amp	(−)ip_c x10^{-5} Amp	ip_a/ip_c	E' volt	$Ep_c/2$	Da x10^{-5} cm^2.s^{-1}	Dc x10^{-5} cm^2.s^{-1}	αn_a	Ks C cm.s^{-1}	Γ c x10^{-9} mol.cm^{-2}	(-) Qc x10^{-5} C	Γ a x10^{-9} mol.cm^{-2}	Q_a x10^{-5} C
9.65	1.61	0.466	-0.005	0.471	5.42	1.28	4.24	0.2305	0.045	45.4	2.53	0.977	1.86	4.44	1.35	18.81	5.70
9.49	3.16	0.483	0.002	0.481	5.32	1.00	5.31	0.2425	0.04	45.2	1.60	1.28	1.87	3.48	1.05	18.47	5.60
9.35	4.67	0.501	-0.001	0.502	5.17	0.943	5.48	0.25	0.042	43.995	1.46	1.14	2.05	3.27	0.992	17.94	5.44
8.93	8.93	0.497	0.009	0.488	4.85	0.459	10.58	0.253	0.034	42.5	0.379	1.95	1.20	1.59	0.482	16.85	5.10
8.20	16.4	0.584	-0.002	0.586	3.45	0.353	9.77	0.291	0.022	25.5	0.267	2.03	2.60	1.22	0.371	11.97	3.63
7.58	22.7	0.628	0.003	0.625	3.37	0.109	30.77	0.3155	0.015	28.4	0.03	4.07	1.79	0.38	0.115	11.69	3.54

Table 7: results of different scan rates on the kinetic and solvation parameters of 1M:1L (Mn-favipiravir) complex for first redox peaks at 305.15K.

υ V.S^{-1}	Ep_a volt	Ep_c volt	ΔEp volt	ip_a x10^{-5} Amp	$(-)$ ip_c x10^{-5} Amp	ip_a/ip_c	E˚ Volt	$Ep_c/2$	Da x10^{-5} cm^2.s^{-1}	Dc x10^{-5} cm^2.s^{-1}	$\alpha n a_c$	Ks C x10^{-1} cm.s^{-1}	Γ c x10^{8} mol.cm^{-2}	(-) Qc x10^{-5} C	Γ a x10^{-8} mol.cm^{-2}	Q a x10^{-5} C
0.1	1.06	0.839	0.221	4.28	3.47	1.23	0.9495	0.908	33.05	21.72	0.708	4.31	1.20	3.65	1.49	4.50
0.02	0.989	0.855	0.134	2.00	1.69	1.18	0.922	0.911	35.95	25.75	0.872	1.02	2.93	8.89	3.47	10.5
0.01	0.956	0.839	0.117	1.36	1.19	1.14	0.8975	0.901	33.13	25.51	0.788	0.580	4.13	12.5	4.70	14.3

Table 8: Results of different scan rates on the kinetic and solvation parameters of 1M:1L (Mn-favipiravir) complex for second redox peaks at 305.15K.

υ V.S^{-1}	Ep_a volt	Ep_c volt	ΔEp volt	ip_a x10^{-5} Amp	$(-)ip_c$ x10^{-5} Amp	ip_a/ip_c	E˚ Volt	$Ep_c/2$	Da x10^{-5} cm^2.s^{-1}	Dc x10^{-5} cm^2.s^{-1}	$\alpha n a_c$	Ks C cm.s^{-1}	Γ c x10^{8} mol.cm^{-2}	(-) Qc x10^{-5} C	Γ a x10^{-8} mol.cm^{-2}	Q a x10^{-5} C
0.1	0.497	0.009	0.488	4.85	0.459	10.58	0.253	0.034	42.49	0.379	1.95	1.20	0.159	0.482	1.68	5.10
0.02	0.375	0.022	0.353	2.33	0.423	5.50	0.1985	0.088	48.81	1.61	0.74	0.188	0.733	2.22	4.04	12.2
0.01	0.339	0.009	0.33	1.22	0.417	2.93	0.174	0.104	26.98	3.14	0.514	0.124	1.45	4.39	4.25	12.9

Table 9: Stability constant (Log βj) and Gibbs free energy change (ΔG) of (Mn-favipiravir) complex for first peak.

[M] x10^{-4} mol	[L] x10^{-4} mol	E°_M volt	E°_C volt	ΔE volt	J(L/M)	Log βj	ΔG (KJ/mol)
9.65	1.61	0.878	0.962	0.084	0.17	2.02	-11.8
9.49	3.16	0.878	0.9535	0.0755	0.33	2.41	-14.1
9.35	4.67	0.878	0.953	0.075	0.5	2.90	-16.97
8.93	8.93	0.878	0.9495	0.0715	1	4.23	-24.71
8.20	16.4	0.878	0.9405	0.0625	2	6.60	-38.6
7.58	22.7	0.878	0.962	0.084	3	9.32	-54.44

Table 10: Stability constant (Log βj) and Gibbs free energy change (ΔG) of (Mn-favipiravir) complex for the second peak

[M] x10^{-4} mol	[L] x10^{-4} mol	E°_M volt	E°_C volt	ΔE volt	J(L/M)	Log βj	ΔG (KJ/mol)
9.65	1.61	0.123	0.2305	0.1075	0.17	2.41	-14.07
9.49	3.16	0.123	0.2425	0.1195	0.33	3.14	-18.35
9.35	4.67	0.123	0.25	0.127	0.5	3.76	-21.98
8.93	8.93	0.123	0.253	0.13	1	5.196	-30.36
8.20	16.4	0.123	0.291	0.168	2	8.34	-48.76
7.58	22.7	0.123	0.3155	0.1925	3	11.11	-64.91

Table 11: Effect of different scan rates on stability constant and Gibbs free energy change of (Mn-favipiravir) complex at (1:1) molar ratio for the first peak

υ v.s^{-1}	[M] x10^{-4} mol	[L] x10^{-4}mol	E°_M volt	E°_C volt	ΔE(v)	J(L/M)	Log βj	ΔG(KJ/mol)
0.1	8.93	8.93	0.878	0.9495	0.0715	1	4.23	-24.71
0.02	8.93	8.93	0.8485	0.922	0.0735	1	4.26	-24.91
0.01	8.93	8.93	0.797	0.8975	0.1005	1	4.71	-27.51

Table 12: Effect of different scan rates on stability constant and Gibbs free energy change of (Mn-favipiravir) complex at (1:1) molar ratio for the second peak.

υ v.s^{-1}	[M] x10^{-4} mol	[L] x10^{-4} mol	E°_M volt	E°_C volt	ΔE(v)	J(L/M)	Log βj	ΔG(KJ/mol)
0.1	8.93	8.93	0.123	0.253	0.13	1	4.263	-24.907
0.02	8.93	8.93	0.125	0.1985	0.0735	1	5.199	-30.359
0.01	8.93	8.93	-0.005	0.174	0.179	1	6.005	-35.087

References

1. G.J. Islam, H.M.N. Akhtar, M.A. Mamun, M.Q. Ehsan, (2009) Investigations on the redox behaviour of manganese in manganese(II)–saccharin and manganese(II)–saccharin– 1,10-phenanthroline complexes, *Journal of Saudi Chemical Society*, **13** 177-183.
2. K.J. Horning, S.W. Caito, K.G. Tipps, A.B. Bowman, M. Aschner, (2015) Manganese Is Essential for Neuronal Health, Annu Rev Nutr, **35** 71-108.
3. U.S. Erdemir, S. Gucer, (2016) Assessment of in vitro bioaccessibility of manganese in wheat flour by ICP-MS and on-line coupled with HPLC, *J. Cereal Sci*., **69** 199-206.
4. J.L. Greger, (1998) Dietary standards for manganese: overlap between nutritional and toxicological studies, *J. Nutr*., **128** 368S–371S.
5. R.C. Maurya, P. Bohre, S. Sahu, M.H. Martin, A.K. Sharma, (2016) Manganese(II) chelates of bioinorganic and medicinal relevance: Synthesis, characterization, antibacterial activity and 3D-molecular modeling of some penta-coordinated manganese(II) chelates in O,N-donor coordination matrix of β-diketoenolates and picolinate, Arabian *Journal of Chemistry***, 9** S54-S63.
6. B. Ali, M.A. Iqbal, (2017) Coordination Complexes of Manganese and Their Biomedical Applications, Chemistry Select, **2** 1586-1604.
7. C.S. Allardyce, P.J. Dyson, (2016) Metal-based drugs that break the rules, Dalton Trans, **45** 3201–3209.
8. D.H. Goldhill, A.J.W.t. Velthuis, R.A. Fletcher, P. Langat, M. Zambon, A. Lackenby, W.S. Barclay, (2018) The mechanism of resistance to favipiravir in influenza, Proc Natl Acad Sci U S A, **115** 11613-11618.
9. T. Baranovich, S.-S. Wong, J. Armstrong, H. Marjuki, R.J. Webby, R. G., (2013) T-705 (Favipiravir) Induces Lethal Mutagenesis in Influenza A H1N1 Viruses In Vitro, *Journal of Virology*, **87** 3741–3751.
10. O.F. Akinyele, E.G. Fakola, O.E. Oyeneyin, O.O. Adeboye, A.O. Ayeni, J.S. Amoko, T.A. Ajayeoba, (2020) Molecular Docking Study of Primaquine-Favipiravir Based Compounds as Potential Inhibitors of COVID-19 Main Protease, European Reviews of Chemical Research, **7** 3-15.
11. M.N.A. El-Hady, E.A. Gomaa, A.G. Al-Harazie, (2019) Cyclic voltammetry of bulk and nano CdCl2 with ceftazidime drug and some DFT calculations, Mol.Liq., **276** 970-985.
12. M. Nazir, R. Khattak, M. S. Khan, I. I. Naqvi, (2021) Study of the histidine complex of uranium(IV): synthesis, spectrophotometric, magnetic and electrochemical properties, Bulletin of the Chemical Society of Ethiopia, **34** 557-569.
13. N.m. Elgrishi, K.J. Rountree, B.D. McCarthy, E.S. Rountree, T.T. Eisenhart, J.L. Dempsey, (2017) A Practical Beginner's Guide to Cyclic Voltammetry, *J. Chem. Educ.*, **95** 197-206.
14. R. Gupta, J. Gamare, M.K. Sharma, J.V. Kamat, (2016) Electrochemical investigations of Pu(IV)/Pu(III) redox reaction using graphene modified glassy carbon electrodes and a comparison to the performance of SWCNTs modified glassy carbon electrodes, Electrochimica Acta, **191** 530-535.
15. M.N.A. El-Hady, E.A. Gomaa, R.R. Zaky, A.I. Gomaa, Synthesis, (2020).characterization, computational simulation, cyclic voltammetry and biological studies on Cu(II), Hg(II) and Mn(II) complexes of 3-(3,5-dimethylpyrazol-1-yl)-3-oxopropionitrile, Mol.Liq., 305
16. E.A. Gomaaa, M.N.A. Hadya, M.H. Mahmoudb, D.A.E. Kot, (2019) Cyclic Voltammetry of Aqueous $CoCl_2$ in the Presence of Ceftriaxone Disodium Salt (Cefs) at 298.65 K, Adv *J Chem A* **2** 1-13.
17. D.S.K. Cook, D.B.R. Horrocks, (2016) Heterogeneous Electron-Transfer Rates for the Reduction of Viologen Derivatives at Platinum and Bismuth Electrodes in Acetonitrile, ChemElectroChem, **4** 320-331.
18. R.J. Klingler, J.K. Kochi, (1981) Electron-Transfer Kinetics from Cyclic

Voltammetry. Quantitative Description of electrochemical reversibility., *J. Phys. Chem*, **85** 1731-1741.
19. A.S.A. Khan, R. Ahmed, M.L. Mirza, (2009) Evaluation of kinetic parameters of uranyl acetate complexes in ethanolic solution by cyclic voltammetry, *J. Radioanal. Nucl. Chem.*, **283** 527-531.
20. S.E. El-Shereafy, E.A. Gomaa, A.M. Yousif, A.S.A. El-Yazed, (2017) Electrochemical and Thermodynamic Estimations of the Interaction Parameters for Bulk and Nano-Silver Nitrate (NSN) with Cefdinir Drug Using a Glassy Carbon Electrode, Iranian *Journal of Materials Science & Engineering*, **14** 48-57.
21. E.A. Gomaa, M.A. Morsi, A.E. Negm, Y.A. Sherif, (2017) Cyclic voltammetry of bulk and nano manganese sulfate with Doxorubicin using glassy Carbon electrode, J.Nano Dimens **8**89-96.
22. J.H. Nelson, (1994) Cyclic Voltammetry; Simulation and Analysis of Reaction Mechanisms, synth. React. Inorg. Met.-org. Chem., **24** 1237-1238.
23. L. WEN-ZHI, L. YOU-QIN, H. GUANG-QI, (2009) Preparation of manganese dioxide modified glassy carbon electrode by a novel film plating/cyclic voltammetry method for H_2O_2 detection, *J. Chil. Chem. Soc*, **54** 366-371.
24. M.M.E. DUARTE, A.S. PILLA, C.E. MAYER, (2003) Electrooxidation of Mn(II) to MnO_2 on graphite fibre electrodes, *Journal of Applied Electrochemistry*, **33** 387–392.
25. J. Singh, A.N. Srivastav, N. Singh, A. Singh, (2019) Stability Constants of Metal Complexes in Solution, 1-18.